

Osmotic coefficients of non-aqueous electrolyte solutions at thermodynamic and McMillan-Mayer level

J. Barthel and R. Neueder

Institut für Physikalische und Theoretische Chemie der Universität Regensburg,
 Universitätsstraße 31, D-8400 Regensburg, Germany

W. Kunz

Laboratoire d'Electrochimie, Université Pierre et Marie Curie, 8 rue Cuvier, 75005 Paris, France.

Abstract – Precise osmotic coefficients from absolute vapor pressure measurements on various electrolyte solutions of organic solvents are given as the reference data for use in relative vapor pressure measurement methods. The availability of reliable data is used for a study of the interdependence of thermodynamic properties and theoretical and experimental McMillan-Mayer level methods, such as chemical model and hypernetted chain calculations and small angle neutron scattering experiments.

INTRODUCTION

The best methods for the determination of osmotic coefficients from very low electrolyte concentrations to saturation are vapor pressure measurements. One of the most frequently applied techniques is the isopiestic method (ref. 1). The drawback of this indirect method is the requirement of reference data which must be measured by absolute methods. Since 1980 a systematic study in our laboratory has provided the reference data for various organic solvent systems for practical use (refs. 2–6).

Vapor pressure measurements yield osmotic coefficients at the model-free macroscopic (or thermodynamic) level. The information at this level are the data sets themselves, which are the input data needed for chemical engineering.

On the other hand, the availability of reliable osmotic coefficients at thermodynamic level from low concentration to saturation for a variety of non-aqueous solutions is a solid base for the study of electrolyte solution models. Most of our actual information on electrolyte solutions is based on Hamiltonian models at the McMillan-Mayer (MM) level. The solvent is considered as a homogeneous and isotropic medium in which the ions are imbedded. Theoretical methods at this level are based on statistical mechanics, such as the chemical model (CM) concept or the hypernetted chain equation (HNC). Experimental techniques situated at this level are static and dynamic light scattering and small angle neutron scattering (SANS). They permit the determination of ion-ion correlation functions directly from the measurements via structure factors, provided that the ions have sufficiently mass. The interdependence of thermodynamic and MM levels will be shown in this paper by the comparison of osmotic coefficients obtained from various methods.

OSMOTIC COEFFICIENTS AT THE THERMODYNAMIC LEVEL

For salt solutions the vapor pressure of the electrolyte E dissolved in the solvent S can be neglected. The gas phase is treated as the real pure gas S with the second virial coefficient $B_s^{*(g)}$ permitting the calculation of the solvent activity a_s from the decrease of the solvent vapor pressure Δp at electrolyte molality m [$mol\ kg^{-1}$] (ref. 2)

$$\ln a_s = \ln\left(1 - \frac{\Delta p}{p^*}\right) + \left(\frac{V_s^{*(l)} - B_s^{*(g)}}{RT}\right) \Delta p, \quad \Delta p = p^* - p, \quad (1\ a,b)$$

where $V_s^{*(l)}$ is the molar volume of the pure liquid solvent, p and p^* are the vapor pressure of the liquid phase at electrolyte concentration m and zero (pure solvent). The osmotic coefficient Φ on the molality scale for the solution of a 1:1-electrolyte is given by the relation (M_s : molar mass of the solvent)

$$\Phi = -\frac{\ln a_s}{2mM_s}. \quad (2)$$

Precise absolute vapor pressure measurements are executed in our laboratory with the help of equipment which is described in ref. 7. Actually reference data at 25°C of about 20 electrolyte solutions of methanol (refs. 2,3), ethanol (ref. 4), acetonitrile (ref. 4), and 2-propanol (ref. 4) are known at concentrations ranging from 0.03 $mol\ dm^{-3}$ to saturation.

The reproduction of the measured osmotic coefficients for use in chemical engineering and technical chemistry can be advantageously carried out with the help of Pitzer's equations (refs. 8–10)

$$\Phi - 1 = f^\Phi + mB^\Phi + m^2C^\Phi, \quad f^\Phi = -\frac{A^\Phi\sqrt{I}}{1+b\sqrt{I}}, \quad I = \frac{1}{2} \sum m_i z_i^2, \quad \text{and} \quad (3\ a,b,c)$$

$$A^\Phi = \frac{1}{3} \sqrt{2\pi N_A d^* \left(\frac{e^2}{4\pi\epsilon_0\epsilon^* kT}\right)^3}, \quad B^\Phi = \beta^{(0)} + \beta^{(1)}e^{-\alpha_1\sqrt{I}} + \beta^{(2)}e^{-\alpha_2\sqrt{I}}, \quad (3\ d,e)$$

where N_A is Avogadro's number, e is the elementary charge, k is the Boltzmann constant, d^* and ϵ^* are the density and permittivity of the pure solvent, z_i is the charge number of ion i , and b , $\beta^{(0)}$, $\beta^{(1)}$, $\beta^{(2)}$, α_1 , α_2 and C^Φ are adjustable parameters. Experience shows that the parameters b , α_1 and α_2 can be kept constant for classes of electrolyte solutions, reducing the numbers of parameters which must be individually adjusted for an electrolyte solution to four (ref. 3).

Table 1 gives a survey on the Pitzer parameters of all investigated non-aqueous solutions permitting the reproduction of the measured data with a precision of about 1% (refs. 2-4).

TABLE 1. Parameters of eqs. 3 at 25°C

	$\beta^{(0)}$	$\beta^{(1)}$	$\beta^{(2)}$	C^Φ	α_2	σ	range
Methanol:							
NaI	0.305321	0.195320	0	-0.043781	0	0.008	0.02-0.8
NaBr	0.105766	0.557814	0	0.083476	0	0.002	0.04-0.7
NaClO ₄	0.135468	0.200269	0	0.009567	0	0.005	0.06-1.3
KI	0.001875	0.553097	0	0.108971	0	0.006	0.02-0.7
RbI	0.054520	0.085276	0	0.020028	0	0.004	0.02-0.4
Et ₄ NBr	0.146567	-0.809858	2.555170	-0.034322	10	0.009	0.04-1.9
Pr ₄ NBr	0.138803	-0.537011	3.347270	-0.019438	10	0.005	0.07-1.6
Bu ₄ NI	0.123951	-1.336730	-3.107380	-0.071479	10	0.004	0.04-0.9
Bu ₄ NBr	0.108319	-0.361489	0.222213	0.000797	10	0.005	0.04-1.7
Bu ₄ NClO ₄	-0.002388	-2.115999	-11.41720	-0.017808	15	0.007	0.05-2.5
Ethanol:							
NaI	0.153991	0.6198422	0.9173275	0.0731329	10	0.014	0.04-1.9
2-Propanol:							
NaI	0.099940	0.8397516	-0.181738	0.0188331	10	0.009	0.06-0.8
Acetonitrile:							
NaI	-0.015102	0.007456	0	0.015844	0	0.006	0.06-1.5
Et ₄ NBr	2.284410	-5.665390	13.9328	-2.488500	10	0.008	0.04-0.4
Pr ₄ NBr	0.042074	-0.734840	2.07255	-0.026001	10	0.007	0.04-1.6
Bu ₄ NI	-0.055027	-0.327851	-8.70830	0.012212	10	0.008	0.05-2.4
Bu ₄ NBr	0.072603	-0.608572	6.25148	-0.025965	10	0.010	0.02-2.0
Bu ₄ NCl	0.040221	-0.310654	3.96707	-0.003887	10	0.010	0.05-2.5

A^Φ : 1.294076 (Methanol), 2.00537 (Ethanol), 2.81616 (2-Propanol), 1.11204 (Acetonitrile)

$\alpha_1 = 2$, $b = 3.2$ for all solvents

Units: A^Φ , α_1 , α_2 , b ($\sqrt{\text{kg/mol}}$); $\beta^{(0)}$, $\beta^{(1)}$, $\beta^{(2)}$ (kg/mol); C^Φ (kg^2/mol^2)

CALCULATION OF OSMOTIC COEFFICIENTS AT THE MM LEVEL

The Gibbs-Duhem equation for an electrolyte solution at molality m and mean activity coefficient γ_{\pm} of a 1:1-electrolyte can be transformed with the help of eq.(2) to

$$d(m\Phi) = m \, d \ln(m\gamma_{\pm}), \quad \gamma_{\pm} = \alpha \gamma'_{\pm} \quad (4a,b)$$

Eq.(4b) splits up the activity coefficient γ_{\pm} of the solute into two parts, the degree of dissociation α and the activity coefficient γ'_{\pm} of the 'free' ions in the solution. This division follows from the assumption of an equilibrium of cations C^+ and anions A^- and ion pairs $[C^+A^-]^0$ (or undissociated electrolyte molecules CA) in the solution

$$C^+ + A^- = [C^+A^-]^0, \quad K_A^{(m)} = \frac{1 - \alpha}{\alpha^2 m} \frac{\gamma_0}{\gamma'_{\pm}{}^2}, \quad (5a,b)$$

and extends the application of eq.(4a) to partially associated or incompletely dissociated electrolytes (ref. 2).

The integration of eq.(4a) yields the relations that express the osmotic coefficient Φ as a function of the activity coefficient γ_{\pm}

$$\Phi(m) = 1 + \frac{1}{m} \int_0^m m \, d \ln \gamma_{\pm}. \quad (6)$$

Eq.(6) is the starting equation of the CM calculations for osmotic coefficients, when the theoretical activity coefficient γ_{\pm} of the CM is inserted.

The CM is a Hamiltonian model taking into account long-range and short-range interactions in the solution by superposition of a Coulombic ($W_{ij}^c(r)$) and a non-Coulombic ($W_{ij}^*(r)$) mean force potential

$$W_{ij}(r) = W_{ij}^c(r) + W_{ij}^*(r). \quad (7)$$

This model subdivides the space around an ion into three regions (refs. 11,12):

- (i) $r \leq a$, a being the minimum distance of two oppositely charged ions, which is assumed to be the sum of effective cation and anion radii, $a = a_+ + a_-$, and
- (ii) $a \leq r \leq R$, within which a paired state of oppositely charged ions, the so-called ion pair, suppresses the long-range interactions with other ions in the solution, where $a \leq r \leq R$ is the region of the non-Coulombic potential W_{ij}^*

$$W_{ij}^*(r) \begin{cases} = \infty & r < a \\ = W_{ij}^* & a \leq r \leq R \\ = 0 & r \geq R \end{cases} \quad (8)$$

The cutoff distance R of the short range cation-anion interactions is generally identified with the upper limit of ion-pair association. Chemical evidence requires us to set $R = a_+ + a_- + n \cdot s$ where s is the length of an orientated solvent molecule and $n = 0, 1$ or 2 .

The relevant quantities of the CM for the calculation of the osmotic coefficient, γ'_{\pm} and $K_A^{(m)}$ are given by the relations (5b) and (9)

$$\ln \gamma'_{\pm} = -\frac{\kappa q}{1 + \kappa R} + \ln \frac{d/d^*}{1 + m M_E}, \quad \ln \gamma_0 = 0, \quad (9 \text{ a,b})$$

$$q = \frac{e^2}{8\pi \epsilon_0 \epsilon^* kT}, \quad \kappa^2 = 16\pi q N_A \alpha c, \quad c = \frac{m d}{1 + m M_E}, \quad (9 \text{ c,d,e})$$

where d and d^* are the density of the solution at molality m and zero (pure solvent), M_E is the molar mass of the electrolyte, and the other symbols were already explained.

The association constant $K_A^{(m)}$ is generally used for application of the CM equation to the measurements. It can also be written in terms of the CM potentials (ref. 12)

$$K_A^{(m)} = 4\pi N_A d^* \exp\left[-\frac{\Delta G_A^*}{RT}\right] \int_0^R r^2 \exp\left[\frac{2q}{r}\right] dr, \quad \Delta G_A^* = N_A W_{+-}^* \quad (10 \text{ a,b})$$

In eqs.(10) ΔG_A^* can be understood as the non-Coulombic part of the Gibbs energy of ion-pair formation.

It is a feature of the CM that the distance parameter R and the association constant K_A are independent of the solution property which was chosen for their experimental determination, and therefore may be used for the prediction of other properties of this electrolyte solution without the necessity of further measurements (refs. 12-14). Fig.1 shows the simulation of osmotic coefficients with the help of the association constant from conductivity data. The data base ELDAR successfully makes use of this feature for data simulations (refs. 15,16).

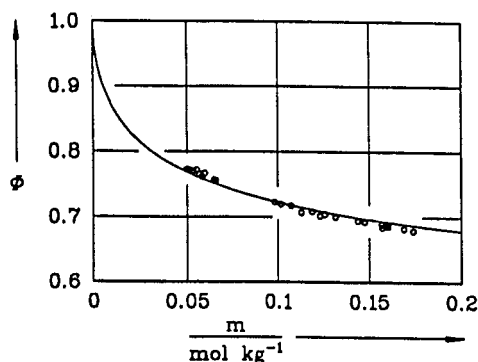


Fig.1. Simulation of the osmotic coefficient Φ of Bu_4NI solutions in methanol at 25°C with the help of CM calculations. Eqs.(6),(4b),(5),(9), using $K_A=43.7 \text{ dm}^3\text{mol}^{-1}$ from conductivity measurements (ref. 33) and $R = a_+ + a_- + s = 1.184 \text{ nm}$ (ref. 12).

CM calculations predict the osmotic coefficient up to 0.1 M solutions at a precision of 1% when the distance parameter R and the ΔG_A^* -data are known.

The integral equation methods like HNC at MM level are related to the macroscopic (thermodynamic) level by means of the virial equation of state

$$\Phi^{MM} = 1 - \frac{1}{6kT\rho} \sum \rho_i \rho_j \int_0^\infty r \frac{\partial u_{ij}(r)}{\partial r} g_{ij}(r) 4\pi r^2 dr, \quad \Phi^{MM} = \frac{\Pi}{kT\rho}, \quad \rho = \sum \rho_i. \quad (11 \text{ a,b,c})$$

Φ^{MM} is the osmotic coefficient in the equilibrium state of the solution characterized by the variables ρ (particle density), T (temperature), $p = p_0 + \Pi$ (p_0 , external pressure; Π , osmotic pressure). Experiments at the thermodynamic level yield osmotic coefficients Φ in the Lewis-Randall system characterized by the variables m (molality), T (temperature), $p = p_0$ (generally the standard pressure 10^5 Pa). Conversion is carried out by the relation (ref. 17)

$$\Phi^{MM} = \Phi (1 + m M_E) \frac{d^*}{d}. \quad (12)$$

Integral equation methods assume interaction potentials of the type

$$u_{ij}(r) = u_{ij}^*(r) + \frac{z_i z_j e^2}{4\pi \epsilon_0 \epsilon^*} \cdot \frac{1}{r}, \quad (13)$$

where $u_{ij}^*(r)$ is a short-range contribution which is either a step potential or a continuous potential.

The step potential (refs. 19,20) is analogous to that of the CM for $W_{ij}(r)$, eq.(8), and also uses the quantities W_{ij}^* ($i, j = +$ or $-$) as adjustable parameters. The HNC parameters show the same pattern as the CM parameters, see Fig.2. Acetonitrile solution data are correlated by a common straight line, in contrast to methanol solutions where two lines are needed, one for alkali metal salt solutions, the other one for tetraalkylammonium salt solutions. Such different behaviour is also known from other CM studies as the result of the interaction of the lone electron pair of methanol oxygen with alkali metal ions and the solvophobic effect of the big tetraalkyl ammonium ions (ref. 20).

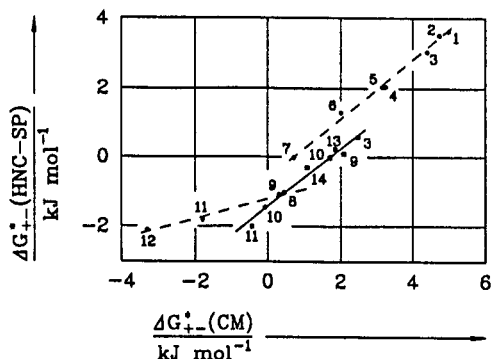


Fig.2. Correlation of the non-Coulombic interaction energies $\Delta G_{+-}^* = N_A W_{+-}^*$ from low concentration CM and HNC step potentials carried out for every salt at equal cutoff distances $R_{+-} = a_+ + a_- + s$. Full points and broken lines: methanol solutions; squares and full line: acetonitrile solutions; 1:NaCl, 2:NaBr, 3:NaI, 4:NaClO₄, 5:KI, 6:RbI, 7:CsI, 8:Et₄NBr, 9:Bu₄NBr, 10:Pen_t₄NBr, 11:Bu₄NI, 12:Bu₄NClO₄, 13:Bu₄NCl, 14:Pr₄NBr.

According to Friedmann et. al. (refs. 21-23) the continuous short-range potential $u_{ij}^*(r)$ can be modelled by the sum of a repulsive potential $COR_{ij}(r)$, a cavity term $CAV_{ij}(r)$, and a Gurney term $GUR_{ij}(r)$, $u_{ij}^*(r) = COR_{ij}(r) + CAV_{ij}(r) + GUR_{ij}(r)$. The repulsive potential is a soft core potential in r^{-9} . The cavity term $CAV_{ij}(r)$ is a potential decreasing as r^{-4} so as to reflect the polarization effects in spherical cavities around the ions. These two potentials use the ionic radii a_i and a_j as the distance parameters. The Gurney term $GUR_{ij}(r) = A_{ij}(V_{mu}/V_s^*)$, results from the overlap of the solvation spheres (Gurney spheres) if two ions have approached one another to distances less than the radii of their solvation spheres, $R_i = a_i + n_i s$ and $R_j = a_j + n_j s$; $V_{mu}(R_i, R_j, r)$ is the overlap volume at a center-to-center distance r of the ions, V_s^* is the molar volume of the pure solvent, and A_{ij} are the Helmholtz energies to transfer the solvent from the overlap region to the bulk solvent.

The Helmholtz energies A_{ij} are the adjustable parameters of the Friedman-Gurney model, generally arbitrarily chosen to fit the experimental osmotic coefficients. Their non-Coulombic parts are not the results of explicit averaging over the solvent properties. They can be considered as 'effective' empirical potentials at the MM level whose parameters are flexible enough for a satisfactory data reproduction. Nevertheless, such 'arbitrary' potentials do not merely serve to represent the experimental data; statistical mechanics provides a link between these MM potentials and ion-ion correlation functions yielding the information on the solution structure.

Integral equation techniques directly link the interaction potential $u_{ij}(r)$ to the pair-correlation function $g_{ij}(r)$ (refs. 20,21,24)

$$g_{ij}(r) = \exp \left[-\frac{u_{ij}(r)}{kT} + \Upsilon_{ij}(r) \right], \quad kT \Upsilon_{ij}(r) = u_{ij}(r) - W_{ij}(r). \quad (14a,b)$$

The HNC equation successfully approximates Υ_{ij} with the help of the total and direct correlation functions, $h_{ij}(r)$ and $c_{ij}(r)$

$$\Upsilon_{ij}(r) = h_{ij}(r) - c_{ij}(r) = \sum \rho_k \int c_{ik}(r_{13}) h_{kj}(r_{32}) d\vec{r}_3. \quad (15)$$

The total correlation function $h_{ij}(r)$ is related to the pair-correlation function $g_{ij}(r)$, $h_{ij}(r) = g_{ij}(r) - 1$; the direct correlation function $c_{ij}(r)$ is defined by the Ornstein-Zernicke equation.

Eqs.(14) can be solved iteratively for $g_{ij}(r)$ as a function of $u_{ij}(r)$. Convergency problems due to Coulombic interactions are overcome with the help of appropriate changes of the original HNC algorithm (refs. 5,25).

A critical judgement on the MM-level calculations must take into account that a multitude of MM-level Hamiltonian models can always be found for the same system (refs. 12,26). Fig.3 shows the reproduction of the osmotic coefficient of the system NaBr/methanol with the help of calculations at low electrolyte concentrations and HNC-calculations at high concentrations with a continuous and a step potential.

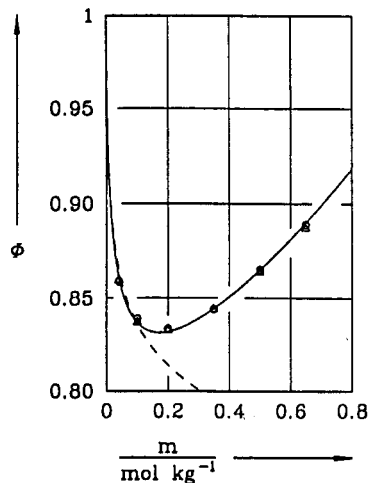


Fig.3. Osmotic coefficients of NaBr in methanol (25°C)
full line: experimental data
broken line: Chemical Model
● HNC Step Potential △ Continuous Potential

When the $g_{ij}(r)$ functions do not correctly correspond to the interaction potentials the calculated free energy results may be incorrect (refs.27,28). A verification by BD (Brownian Dynamics) simulations is then advisable (ref.6), especially for the aqueous solutions of higher charged electrolytes or the low permittivity solutions of small ions.

In some cases osmotic coefficients alone may not be sufficient to determine a unique interaction model. Quite different potential models and hence different sets of $g_{ij}(r)$ can correctly describe osmotic coefficients over wide concentration ranges.

On the other hand, calculated osmotic coefficients are sensitive to slight changes in the potential parameters. This means that models which qualitatively suggest a very similar physical picture may lead to distinctly different osmotic coefficients, especially at higher salt concentrations.

EXPERIMENTAL DETERMINATION OF OSMOTIC COEFFICIENTS AT THE MM LEVEL

The coherent scattering intensity $I(q)$ of the ions in solution is a function of the wave length λ of the incident neutron beam and of the scattering angle Θ which can be related to the so-called wave-number transfer, $q = (4\pi/\lambda) \sin(\Theta/2)$. The scattering intensity directly reflects the MM pair-correlation function $g_{ij}(r)$ (refs. 29-31) via the structure factor $S_{ij}(q)$

$$I(q) = \sum \sum (s_i - s_o) V_i (s_j - s_o) V_j F_i(q) F_j(q) S_{ij}(q), \quad (16 a)$$

where s_i, s_j , and s_o are the scattering length densities of the ions i, j and of the solvent, V_i and V_j are the molar volumes, and

$$F_i(q) = 3 \frac{\sin(qa_i) - qa_i \cos(qa_i)}{(qa_i)^3}, \quad S_{ij}(q) = \rho_i \delta_{ij} + \rho_i \rho_j \frac{4\pi}{q} \int_0^\infty \sin(qr) [g_{ij}(r) - 1] r dr. \quad (16 b, c)$$

$F_i(q)$ is the form factor amplitude of a spherical ion i with radius a_i . The structure factor $S_{ij}(q)$ is the Fourier transform of the MM pair-correlation function $g_{ij}(r)$ and hence can be directly compared to the experimental scattering spectra. However, there is also a direct relation between the osmotic coefficient and the scattering intensity (ref.31). The extrapolation of eqs.(16) to zero wave number transfer, $q \rightarrow 0$, yields the thermodynamic limit

$$I(0) = \sum \sum (s_i - s_o) V_i (s_j - s_o) V_j S_{ij}(0). \quad (17)$$

Electroneutrality requires that $S_{++}(0) = S_{+-}(0) = S_{--}(0) = S(0)$, yielding

$$I(0) = [(s_+ - s_o) V_+ + (s_- - s_o) V_-]^2 S(0) = [(s - s_o) V]^2 S(0), \quad (18)$$

where $V = V_+ + V_-$ is the partial molecular volume of the electrolyte and $s = (s_+ V_+ + s_- V_-)/V$ is its scattering length density. $S(0)$ is related to the osmotic pressure via the osmotic compressibility χ^{osm}

$$S(0) = \frac{1}{4} \rho^2 k T \chi_{p,T}^{osm} = \frac{1}{4} \rho k T \left(\frac{\partial \rho}{\partial \Pi} \right)_{p,T}, \quad \chi^{osm} = \frac{1}{\rho} \left(\frac{\partial \rho}{\partial \Pi} \right)_{p,T}. \quad (19 a, b)$$

Substitution of Π , eq.(11b), in eq.(19a) yields the relation between $I(0)$ and the osmotic coefficient Φ^{MM} (c , molarity [mol dm^{-3}])

$$I(0) = 1000 [(s - s_o) V]^2 N_A c \frac{\partial c}{\partial (c \Phi^{MM})}. \quad (20)$$

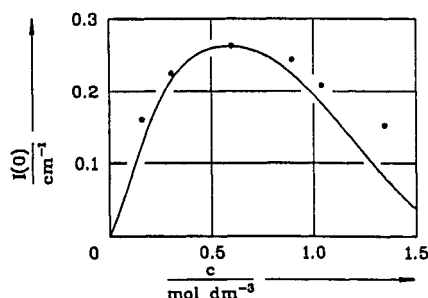


Fig.4. Absolute intensity $I(0)$ of the coherent contribution of n-Pent₄NBr (in 2-PrOH) to neutron scattering at $q=0$ (full points). The full line was calculated from experimental vapor pressure data Φ^{MM} (ref. 31) according to eq.(20).

Fig.4 shows the comparison between $I(0)$ extrapolated from a scattering experiment on solutions of n-Pent₄NBr in 2-propanol and $I(0)$ calculated with the help of eq.(20) from experimental osmotic coefficients determined by vapor pressure measurements (ref. 31). Because of the high precision of the $(\partial c/\partial c\Phi)$ -data from vapor pressure measurements (ref. 31) Fig.4 reflects the accuracy of the absolute scattering measurements showing that precise measurements of osmotic coefficients can be used for exact calibration of scattering data. This is of special interest at high electrolyte concentrations where the contributions from multiple scattering to the neutron spectra are important.

Fig.4 also satisfactorily explains by the comparison with scattering intensities from thermodynamic data the surprising result that the experimental scattering intensities decrease at salt concentrations beyond 0.60 mol dm^{-3} .

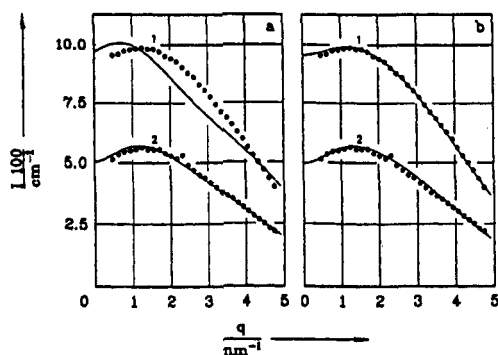


Fig.5. Comparison of the coherent neutron scattering spectra of $\text{Bu}_4\text{NBr}/\text{H}_2\text{O}$ solutions (full points) at electrolyte concentrations of 0.30 mol dm^{-3} (1) and 0.15 mol dm^{-3} (2) with model calculations (full lines 1 and 2). For explanations see the text.

Figs.5 show experimental SANS spectra of aqueous $n\text{-Bu}_4\text{NBr}$ solutions (ref.32). The theoretical curves of Fig.5a are calculated with the help of $g_{ij}(r)$ functions published by Ramanathan et. al. (ref.22) who adjusted the underlying Friedman-Gurney potential to the osmotic coefficients from vapor pressure measurements reported by Ku (ref.33). The predicted scattering intensities at low scattering angle are in good agreement with the measured scattering data. The theoretical curve at the higher electrolyte concentration differs significantly from the experimental one. Another adjustment of the potential parameters which takes into account both the vapor pressure and the scattering data yields the results shown in Fig.5b (ref.32). This comparison illustrates a feature of HNC calculations previously discussed. The knowledge of the concentration dependence of osmotic coefficients is important, but in some cases this reference is insufficient to distinguish between different assumptions on ionic distribution functions and information from other experimental techniques is needed.

Various examples where experimental and theoretical methods are combined with the information from osmotic coefficients are given in refs. 6,30.

REFERENCES

1. R.F.Plaford, in R.M.Pytkowicz (Ed.), Activity Coefficients in Electrolyte Solutions 1, CRC, Boca Raton, 65-79 (1979).
2. J.Barthel, R.Neueder and G.Laueremann, J. Solution Chem. **14**, 621-633 (1985).
3. J.Barthel, G.Laueremann and R.Neueder, J. Solution Chem. **15**, 851-867 (1986).
4. J.Barthel and G.Laueremann, J. Solution Chem. **15**, 869-877 (1986).
5. J.Barthel and W.Kunz, J. Solution Chem. **17**, 399-415 (1988).
6. W.Kunz, J.Barthel, L.Klein, T.Cartailier, P.Turq, and B.Reindl, J. Solution Chem. **20**, 875-891 (1991).
7. J.Barthel and R.Neueder, GIT Fachzeitschr. Labor. **28**, 1002-1012 (1984).
8. K.S.Pitzer, J.Phys.Chem. **77**, 268-277 (1973).
9. K.S.Pitzer, R.N.Roy, and L.F.Sylvester, J.Am.Chem.Soc. **99**, 4930-4936 (1977).
10. K.S.Pitzer and J.C.Peiper, J.Phys.Chem. **84**, 2396-2398 (1980).
11. J.Barthel, Ber.Bunsenges.Phys.Chem. **83**, 634-642 (1979).
12. J.Barthel, H.-J.Gores, G.Schmeer, and R.Wachter, Topics Curr.Chem. **111**, 33-144 (1983).
13. J.Barthel, in P.S.Glaeser (Ed.), The Role of Data in Scientific Progress, Elsevier, North Holland, 337-340 (1985).
14. J.Barthel, in DECHEMA (Ed.), Phase Equilibria and Fluid Properties in the Chemical Industry, Part II, DECHEMA, Frankfurt, 497-507 1980.
15. J.Barthel and H.Popp, J.Chem.Inf.Comput.Sci. **31**, 107-115 (1991).
16. J.Barthel and H.Popp, Anal.Chim.Acta (1992) in press.
17. H.L.Friedman, J.Solution Chem. **1**, 387-412 (1972).
18. J.C.Rasaiah and H.L.Friedman, J.Phys.Chem. **72**, 3352-3353 (1968).
19. J.C.Rasaiah, J.Chem.Phys. **52**, 704-715 (1970).
20. J.Barthel, W.Kunz, G.Laueremann, and R.Neueder, Ber.Bunsenges.Phys.Chem. **92**, 1372-1380 (1988).
21. P.S.Ramanathan and H.L.Friedman, J.Chem.Phys. **54**, 1086-1099 (1971).
22. P.S.Ramanathan, C.V.Krishnan, and H.L.Friedman, J.Solution Chem. **1**, 237-262 (1972).
23. H.Xu, H.L.Friedman, and F.O.Raineri, J.Solution Chem. **20**, 739-773 (1991).
24. W.Kunz and J.Barthel, J.Solution Chem. **19**, 339-352 (1990).
25. A.R.Alnatt, Mol.Phys. **8**, 533-539 (1964).
26. H.L.Friedman, Faraday Discuss.Chem.Soc. **64**, 7-15 (1977).
27. R.Bacquet and P.J.Rossky, J.Chem.Phys. **79**, 1419-1426 (1983).
28. Y.V.Kalyuzhnyi, M.F.Holovko, and A.D.J.Haymet, J.Chem.Phys. **95**, 9151-9164 (1991).
29. W.Kunz, P.Calmettes, and P.Turq, J.Chem.Phys. **92**, 2367-2373 (1990).
30. W.Kunz, P.Turq, M.C.Bellissent-Funel, and P.Calmettes, J.Chem.Phys. **95**, 6902-6910 (1991).
31. W.Kunz, P.Turq, P.Calmettes, J.Barthel, and L.Klein, J.Phys.Chem. **96**, 2743-2749 (1992).
32. P.Calmettes, W.Kunz, and P.Turq, Physica B, in press.
33. J.C.Ku, Ph.D.Thesis, Univ. Pittsburgh (1971).
34. R.L.Kay, C.Zawoyski, and D.F.Evans, J.Phys.Chem. **69**, 4208-4215 (1965).